ELSEVIER

Biochimica et Biophysica Acta 1327 (1997) 5–16

BIOCHIMICA ET BIOPHYSICA ACTA
BBA

Conventional and saturation-transfer EPR of spin-labeled mutant bacteriophage M13 coat protein in phospholipid bilayers

Wim F. Wolkers [a], Ruud B. Spruijt [a], Anita Kaan [b], Ruud N.H. Konings [b], Marcus A. Hemminga [a,*]

[a] *Department of Molecular Physics, Agricultural University, Dreijenlaan 3, 6703 HA Wageningen, Netherlands*
[b] *Department of Molecular Biology, University of Nijmegen, Toernooiveld, 6525 ED Nijmegen, Netherlands*

Received 1 November 1996; revised 7 February 1997; accepted 13 February 1997

Abstract

A mutant of bacteriophage M13 was prepared in which a cysteine residue was introduced at position 25 of the major coat protein. The mutant coat protein was spin-labeled with a nitroxide derivative of maleimide and incorporated at different lipid-to-protein (L/P) ratios in DOPC or DOPG. The rotational dynamics of the reconstituted mutant coat protein was studied using EPR and saturation transfer (ST) EPR techniques. The spectra are indicative for an anisotropic motion of the maleimide spin label with a high order parameter ($S = 0.94$). This is interpreted as a wobbling motion of the spin label with a correlation time of about 10^{-6} to 10^{-5} s within a cone, and a rotation of the spin label about its long molecular axis with a correlation time of about 10^{-7} s. The wobbling motion is found to correspond generally to the overall rotational motion of a coat protein monomer about the normal to the bilayer. This motion is found to be sensitive to the temperature and L/P ratio. The high value of the order parameter implies that the spin label experiences a strong squeezing effect by its local environment, that reduces the amplitude of the wobbling motion. This squeezing effect is suggested to arise from a turn structure in the coat protein from Gly23 to Glu20. © 1997 Elsevier Science B.V.

Keywords: M13 coat protein; (ST)-EPR; Membrane protein; Site-directed spin labeling; Protein dynamics; Protein conformation

1. Introduction

The infection of *Escherichia coli* with the bacteriophage M13 results in the entry of viral DNA into the cytoplasm and storage of the major coat protein in the cytoplasmic membrane. Newly synthesized coat proteins in the cytoplasm are inserted into the cytoplasmic membrane and stored as integral membrane proteins [1–4]. The amino acid sequence of the major coat protein is made up of a central hydrophobic region enclosed by an amphipathic N-terminus and a basic C-terminus. The hydrophobic region is

Abbreviations: CCMV, cowpea chlorotic mottle virus; CD, circular dichroism; DOPC, 1,2-dioleoyl-*sn*-glycero-3-phosphocholine; DOPG, 1,2-dioleoyl-*sn*-glycero-3-phosphoglycerol; DTNB, 5,5″-dithio-bis(2-nitrobenzoic acid); EPR, electron paramagnetic resonance; HPSEC, high-performance size exclusion chromatography; L/P, lipid to protein molar ratio; NMR, nuclear magnetic resonance; SDS, sodium dodecylsulfate; ST-EPR, saturation transfer electron paramagnetic resonance

* Corresponding author. Department of Molecular Physics, Agricultural University, P.O. Box 8128, 6700 ET Wageningen, Netherlands. Fax: +31-317 482725. E-mail: marcus.hemminga@virus.mf.wau.nl

PII S0005-2736(97)00038-2

thought to form the membrane spanning part of the protein when it is stored in the bacterial membrane. In lipid model systems the coat protein can adopt two different conformations that have quite a different aggregation behavior (for reviews see Refs. [5,6]). M13 coat protein in a predominant α-helix conformation can form reversible small aggregates (α-oligomeric protein) and is assumed to be the biological active form in the infection and assembly processes [6,7]. The β-polymeric form is considered to be an artificial state that occurs in reconstituted lipid-protein systems. The present paper will deal with the α-oligomeric form of the major coat protein.

The secondary structure of micellar-bound M13 coat protein has been determined from high-resolution two-dimensional NMR studies [8–11]. From this work it follows that micellar-bound M13 coat protein consists of two α-helical segments (between Pro6 and Glu20 and between Tyr24 and Ser50) linked by a short region of uncertain conformation [9–11]. The longer hydrophobic C-terminal helix seems to be very stable and is proposed to traverse the micelle. The other helix is more structurally labile and is proposed to reside on the outside of the micelle. However, its position relative to the micellar surface is not expected to be fixed. There is probably significant motion, most likely via a hinge region around Ile22 [10]. For membrane-embedded M13 coat protein it is well established that the hydrophobic helix of M13 coat protein is oriented preferentially parallel to the membrane normal [12]. It may be possible that the N-terminal helix, which has an amphipathic nature, is associated parallel to the plane of the bilayer [9]. However, spectroscopic experiments carried out on reconstituted phospholipid systems have not given information about steric effects of N-termini at increasing coat protein concentrations [5,13–15]. Therefore the orientation of the N-terminal part of reconstituted M13 coat protein with respect to the bilayer surface is still a matter of debate.

M13 coat protein does not contain a suitable site for specific labeling the molecule for biophysical studies in a membranous environment. Previously the single Met28 that is located in the hydrophobic region of the protein has been used to spin label the coat protein with a nitroxide derivative of iodoacetamide. Both conventional and saturation transfer (ST) EPR studies were performed to investigate the rotational motions of the protein over a large dynamic range [16]. These results were interpreted in terms of two correlation times representing a long axis rotational diffusion of the protein, and a wobbling motion of the protein within the lipid bilayer. However, the spectra contained a relatively large contribution of non-specific labeling that was limiting the information arising from ST-EPR.

Following the approach of site-directed spin labeling [17], site-directed mutagenesis is employed in the present study to probe the hydrophobic environment of the M13 coat protein when reconstituted in phospholipid model membranes. This is carried out by replacing Ala25 for a cysteine residue, and using a highly specific maleimide spin label for EPR research. The position of the spin label is expected to be close to the border of the membrane in the direct vicinity of the aromatic amino acid residues Tyr21, Tyr24, and Trp26. The aromatic side chains of the amino acids Tyr21, Tyr24, and Trp26 that are buried in the hydrophobic region of the membrane, close to the membrane/water interface, may provide a strong membrane anchoring. This could be a common property of membrane proteins, since aromatic amino acid residues are often found at the membrane/water interface [18–21]. Spin label EPR of mutant coat protein A25C may provide information about the local environment and dynamics of the coat protein, including the orientation of the N-terminal domain. Both conventional and ST-EPR will be used to cover a wide range of molecular motions. Conventional EPR observes molecular motions with rotational correlation times τ_c from 10^{-10} to 10^{-7} s; ST-EPR extends this range in the slow motion region for values of τ_c up to 10^{-3} s.

2. Materials and methods

2.1. Chemicals

The phospholipids DOPC and DOPG were obtained from Avanti Polar lipids (Birmingham, AL, USA). DTNB was obtained from Sigma. The spin label 3-maleimido proxyl was obtained from Aldrich Chemical Co.

2.2. Mutagenesis

Oligonucleotide-directed mutagenesis according to the Kunkel method [22] was performed to introduce a cysteine residue at position 25 into the major coat protein of bacteriophage M13 (A25C). In addition to this mutation, the produced mutant has an additional mutation at position 27: A27S.

2.3. Spin-labeling of mutant M13 coat protein

Bacteriophages M13 (wild type) and mutant M13 (A25C/A27S) were grown and purified as described before [23]. The cholate-isolated coat protein of M13 was prepared by a modification of the procedure of Makino et al. [24]. Typically 4 ml of bacteriophage solution (concentration 17 mg/ml) was mixed with 8 ml of 100 mM sodium cholate, 150 mM NaCl, 0.2 mM EDTA, 10 mM Tris-HCl, pH 7.0, and a few drops of chloroform. The suspension was incubated at 37°C with occasional mixing until a clear non-opalescent solution was obtained. Wild type as well as mutant type of coat protein were spin-labeled with 3-maleimido proxyl. The spin label was directly added in a 2:1 molar ratio of spin label with respect to the protein. The reaction was allowed to proceed for 15 min at room temperature under continuous stirring and stopped by adding excess β-mercaptoethanol. The mixture of disrupted phage and spin label was then applied to a Sephacryl S-300 column and eluted with 10 mM sodium cholate, 150 mM NaCl, 10 mM Tris-HCl, and 0.2 mM EDTA pH 8.0 to separate the viral DNA, and free spin label from the major coat protein. Fractions with absorbance ratio A_{280}/A_{260} greater than 1.4 were collected.

2.4. Lipid-protein reconstitution

From the desired amount of lipid solution, chloroform was evaporated with nitrogen gas and subsequently dried under vacuum for at least 2 h. The phospholipids (DOPC or DOPG) were solubilized in a 50 mM sodium cholate, 150 mM NaCl, 10 mM Tris-HCl, and 0.2 mM EDTA adjusted to pH 8.0 by brief sonication with a Branson Sonifier B15 for 1 min. To this solution the desired amount of spin-labeled protein was added, to obtain L/P ratios in the range from 2 to 400. Reconstitution was achieved by removal of sodium cholate by extensive dialyses at room temperature against a 100-fold excess buffer (150 mM NaCl, 10 mM Tris-HCl, 0.2 mM EDTA, pH 8.0) for a total of 48 h changing the buffer every 12 h. After reconstitution, the samples were concentrated for EPR purposes as described by Sanders et al. [13]. The aggregation and conformational state of the coat protein was checked using HPSEC [23]. The L/P ratios and homogeneity in L/P ratios were determined after sample preparation as described previously [23].

2.5. Conventional EPR

Samples containing spin-labeled mutant M13 coat protein, reconstituted in multilamellar vesicles, were contained in 100 μl glass capillaries, which were accommodated within standard 4 mm diameter quartz EPR tubes. Samples of 5 mm in length were used. EPR measurements were performed on a Bruker ESP 300E EPR spectrometer equipped with 4103 TM microwave cavity and a liquid nitrogen temperature regulation. The EPR settings were: modulation amplitude of 0.05 mT, field centre at 3.48 T with a scan range of 10 mT, and a microwave frequency of 9.8 GHz. The field modulation was 100 kHz, and the scan time was 4 min. The microwave power was 12 mW. The in-phase absorption EPR spectra were accumulated for four scans.

2.6. Saturation transfer EPR

To record ST-EPR spectra of spin-labeled mutant M13 coat protein, 100 μl glass capillaries were filled to exactly 5 mm (5 μl) of sample. Absorption ST-EPR spectra were recorded in the second harmonic in quadrature (90° out-of-phase). Phase setting was achieved using the self-null method [25,26]. The modulation amplitude was 0.5 mT and the modulation frequency was 50 kHz. The glass capillary was fixed in the centre of the cavity. The microwave power was set at 32 mW, adjusted for each sample at each temperature as suggested in a standardized protocol [27]. To obtain effective rotational correlation times from the diagnostic line height ratios, reference spectra were measured under the same experimental conditions as described above, using maleimide spin-labeled hemoglobin in glycerol-water solutions [28].

2.7. Molecular modeling

For molecular modeling of the spin label attached to mutant M13 coat protein (A25C) the computer programme Insight II (Biosym Technologies, San Diego, CA, USA) was used. The modeling was carried out using the standard parameter sets and commands of the programme. First the primary structure of the coat protein mutant was generated. The maleimide spin label was generated and attached to the cysteine. For the extended structure an α-helix was constructed from amino acid 1–50. In the case of the L-shaped structure, an α-helix was constructed from amino acid 1–19 and 24–50, and a β-turn of type B2 [29] from amino acid 20–23.

3. Results

3.1. Protein studies

Oligonucleotide-mediated mutagenesis of the major coat protein of bacteriophage M13 resulted in a viable mutant containing a single cysteine residue at position 25 and an additional replacement of alanine for serine at position 27 (A25C/A27S). The amino acid sequence of the major coat protein of the viable phage mutant was confirmed by automated DNA sequencing. An additional check carried out with the DTNB reaction confirmed the insertion of only one cysteine residue per protein monomer. Although the yield of the mutant phage is lower as compared to that of wild type phage (50 and 150 mg/l, respectively), the presence of phage particles ensures proper functioning of the mutated coat protein in all processes involved in the bacteriophage life cycle, including the membrane-bound state.

The mutant coat protein reconstituted in DOPC vesicles was compared with the wild type M13 coat protein with respect to its conformation, and aggregation properties. SDS-HPSEC elution profiles demonstrated the presence of the coat protein in a monomeric state. This is indicative for an α-oligomeric state of the protein [23]. The mutated M13 coat protein showed an additional fraction (less than 5% of total protein) with a molecular weight twice that of monomeric coat protein. We have ignored the presence of these unlabeled coat protein dimers in our further analyses. No spin labeling of wild type coat protein could be observed, which shows that labeling of the maleimide spin label specifically occurs at the introduced cysteine group. After the EPR experiments the samples were again checked for aggregation. No changes could be detected, showing that the α-oligomeric state of the protein in the model membrane systems was stable at all L/P ratios used.

3.2. Conventional EPR

In Fig. 1 the effect of the L/P ratio on the conventional EPR spectra of spin-labeled mutant M13 coat protein incorporated in DOPC vesicles is shown. The line shape of the EPR spectra at high L/P ratios ($L/P > 35$) suggests that the spin label undergoes a relatively fast anisotropic motion about the principal *z*-axis of the nitroxide g-factor and hyperfine tensors of the maleimide spin label. This is similar as has been observed and computer simulated for spin-labeled fatty acid spin labels incorporated in lipid bilayers [30]. The outer hyperfine splitting $2A_{zz}$ is around 6.3 mT, which is close to the rigid limit value ($2A_{zz} = 6.7$ mT), indicating a high order parameter ($S = 0.94$) of the spin label.

At L/P ratios below 35, there is an increase in line broadening and loss of spectral detail. The spectrum becomes similar to that of an isotropic powder EPR spectrum, suggesting that all motion has slowed down beyond the limit of motional sensitivity of conven-

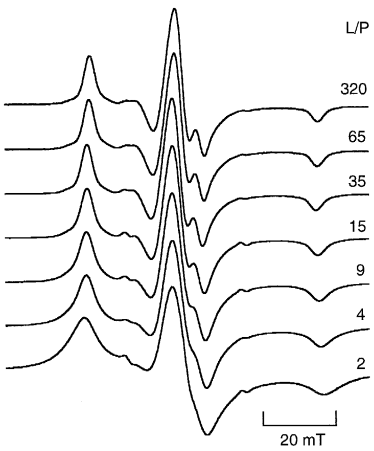

Fig. 1. Conventional EPR spectra of maleimide spin-labeled mutant M13 coat protein (A25C/A27S) in DOPC vesicles at different L/P ratios at a temperature of 25°C.

tional EPR ($\tau_c \approx 10^{-8}$ s). This is illustrated in Fig. 2, were the effect of the L/P ratio on the outer hyperfine splitting $2A_{zz}$, and the linewidths of the low-field (Δ_L) and high-field (Δ_H) lines is presented. As can be seen, a drastic decrease of the outer hyperfine splitting $2A_{zz}$ can be observed at L/P ratios below 35, indicating a strong inhibition of the molecular mobility of the spin label. This effect is also reflected by the linewidths. At L/P 2 there is a very high protein concentration, and it can not be excluded that part of the line broadening is due to spin-spin interaction.

Upon reconstitution of the spin-labeled mutant coat protein into negatively charged DOPG at L/P ratios above 20, there are only minor differences in the EPR line shape as compared to DOPC (data not shown). This indicates that the motional properties of the reconstituted protein are not dependent on the charge of the phospholipid headgroups.

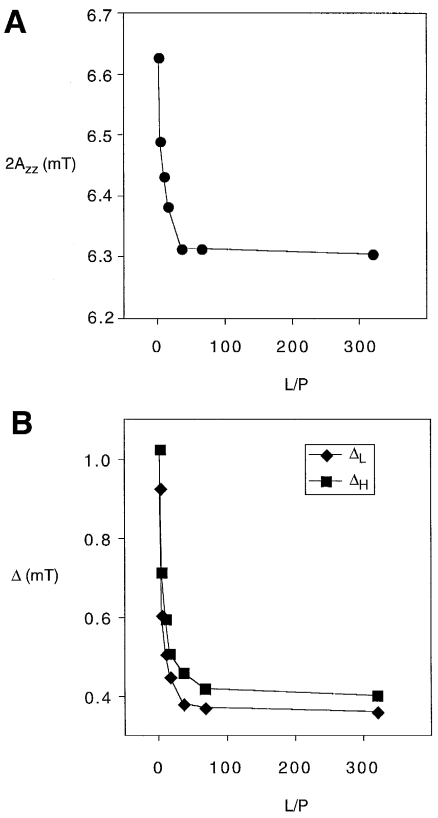

Fig. 2. Outer hyperfine splitting $2A_{zz}$ (A), and half-widths at half-height (B) of the low-field Δ_L and high-field Δ_H lines in conventional EPR spectra of maleimide spin-labeled M13 coat protein as a function of the L/P ratio.

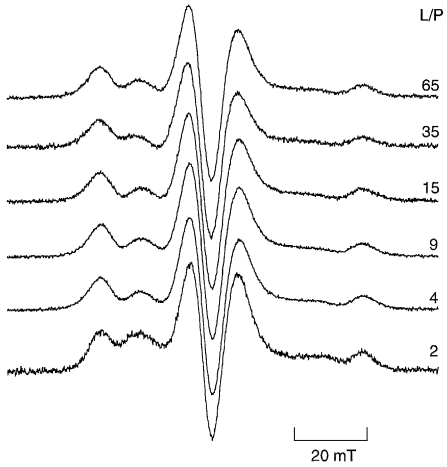

Fig. 3. ST-EPR spectra of maleimide spin labeled mutant M13 coat protein (A25C/A27S) reconstituted in DOPC vesicles at different L/P ratios at a temperature of 20°C.

3.3. ST-EPR

ST-EPR is an excellent method to further study the motional anisotropy and dynamics of the spin-labeled mutant coat protein embedded in phospholipid bilayers. The ST-EPR spectra of maleimide spin-labeled mutant coat protein reconstituted in DOPC vesicles at different L/P ratios are shown in Fig. 3. To analyze the motional characteristics from these spectra, we follow the approach that has been carried out for spin-labeled lipids [31] and spin-labeled CCMV [32]. This method is based on the three diagnostic line-height ratios L″/L, C′/C, and H″/H of the low-field, centre, and high-field part of the ST-EPR spectrum [25]. Anisotropic motion of the maleimide spin label about its principal *z*-axis, as deduced from Fig. 1, modulates only the anisotropy of the g-factor and hyperfine tensors in the principal *x-y* plane, leaving the other tensor components unaffected. Therefore this motion gives rise to saturation transfer in the central part of the ST-EPR spectrum, only affecting C′/C. In contrast, motion of the spin label *z*-axis itself causes saturation transfer throughout the whole spectrum. Thus C′/C yields an estimate for the motion about the principal *z*-axis ($\tau_{\|}$), which approximately coincides with the long spin label axis. The ratios L″/L and H″/H give the correlation time for a wobbling motion of the principal *z*-axis itself ($\tau_{\perp}$) [32]. The relation between isotropic rotational correla-

tion times and the lineheight ratios is carried out with ST-EPR spectra obtained from maleimide spin-labeled hemoglobin [28,32], measured under the same experimental conditions.

The result of this analysis is presented in Fig. 4. The L″/L ratio (Fig. 4A) represents the wobbling motion with a correlation time $\tau_{\perp}$, which varies from about 1×10^{-5} to 6×10^{-7} s for temperatures between 10 and 30°C at L/P 65. The C′/C ratio (Fig. 4B) gives the motion around the long spin label axis with a correlation time $\tau_{\parallel}$, which varies from about 1.4×10^{-7} to 5×10^{-8} s at L/P 65 in the same temperature range. The line height ratio as obtained from the H″/H ratio gives a correlation time in the order of 10^{-5} s. Under our conditions of ST-EPR spectroscopy of maleimide spin-labeled hemoglobin, the ratio H″/H in the calibration set has a low sensitivity for motion, i.e. it is almost independent of the rotational correlation time. Therefore this ratio is not further used in our analysis.

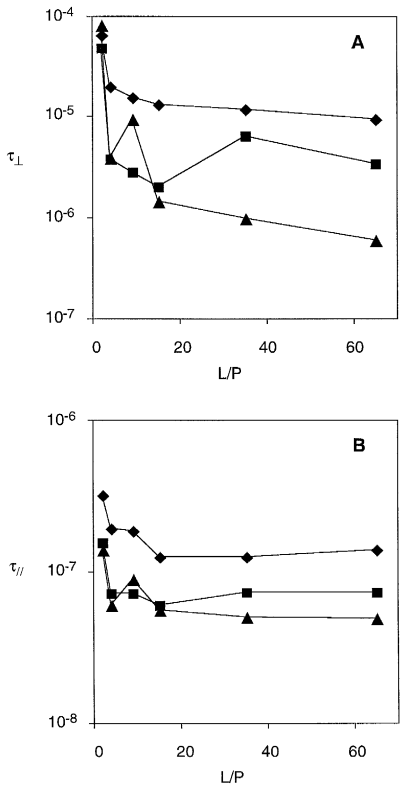

Fig. 4. Correlation times of maleimide spin labeled M13 coat protein as determined from the lineheight ratios in the low field region L″/L ratio (A) and the central region C′/C (B) in the ST-EPR spectrum. The symbols represent temperatures of 10 (♦), 20 (■), and 30°C (▲).

As can be seen in Fig. 4A, $\tau_{\perp}$ strongly increases at decreasing L/P ratios for L/P ratios below 15; this effect is much smaller for $\tau_{\parallel}$ (Fig. 4B). For L/P ratios between 15 and 65 $\tau_{\parallel}$ is almost constant, whereas $\tau_{\perp}$ still has a tendency to decrease. An increase in temperature decreases $\tau_{\parallel}$ and $\tau_{\perp}$, however this effect is 6 times as strong for $\tau_{\perp}$ as compared to $\tau_{\parallel}$.

4. Discussion

Site-directed EPR spin labeling is used in this paper to probe the local molecular motions of M13 coat protein reconstituted into phospholipids. Since wild type M13 coat protein contains no cysteine residue, a cysteine residue is introduced in the hydrophobic region of the protein at position 25 (A25C), close to the aromatic amino acid residues Tyr21, Tyr24, Trp26, and the hinge region around Ile22. The mutant coat protein has an additional mutation in the protein at position 27: A27S, which is probably a compensating effect. Recently, the same strategy was followed by Khan et al. [33]. These authors employed a randomized mutagenesis procedure to generate the M13 mutant Y24C-V31A, which was used to study the intact virion, and the coat protein dissolved in SDS micelles using spin label EPR. Although the yield of the A25C/A27S mutant of M13 bacteriophage is about a factor of 3 lower than the yield of wild type M13 bacteriophage, it indicates that the properties of the coat protein are not largely affected by the mutations. Spin labeling of the mutant coat protein with 3-maleimido proxyl is found to be highly specific for the cysteine group.

The EPR (Fig. 1) and ST-EPR (Fig. 3) spectra of spin-labeled mutant coat protein incorporated in phospholipids at high L/P ratios ($L/P > 35$) are indicative for an anisotropic motion of the maleimide spin label about the principal *z*-axis of the nitroxide g-factor and hyperfine tensors with a high order parameter ($S = 0.94$). As has been discussed previously for the analysis of EPR and ST-EPR spectra of maleimide spin-labeled coat protein of the plant virus CCMV, such an anisotropic motion arises from a

local motion of the maleimide spin label about its *z*-axis, which is almost parallel to the long axis of the spin label [32,34]. In addition, there is an anisotropic rotational motion of the coat protein about the normal to the membrane. This motional model is shown in Fig. 5, which is an adaptation of the model proposed for maleimide spin-labeled CCMV coat protein [32,34]. The main reason for the anisotropic *z*-axis rotation (described with correlation time $\tau_{\parallel}$) is a local effect, arising from the covalent binding of the maleimide moiety to the cysteine side chain. Therefore, this anisotropic rotation is in first instance independent of the location of the cysteine residue in the protein, the type of protein, the secondary structure, and side chains of neighbouring amino acid residues. However, these factors will affect the 'swing-out' amplitude and correlation time $\tau_{\perp}$ of the spin label.

In the model in Fig. 5, it can be seen that as the protein reorientates about the membrane normal, this motion will affect $\tau_{\perp}$ (the arrow shown with $\tau_{\perp}$ is perpendicular to the normal **n**). Also a wobbling motion of the coat protein will influence $\tau_{\perp}$, however, for simplicity our model does not include such a protein wobble, since this is considered to be a minor effect. Therefore the overall protein reorientation about the normal mainly affects $\tau_{\perp}$. It follows from the high value of the order parameter ($S = 0.94$) that the amplitude of the local wobbling spin label motion is small, and in fact the contribution of the local motion to $\tau_{\perp}$ ($\tau_{\perp(\text{local})}$) is negligible, since it is almost 'rigid', i.e. $\tau_{\perp(\text{local})} \gg \tau_{\perp(\text{membrane normal})}$). Thus $\tau_{\perp(\text{membrane normal})}$ takes over all the motional effects.

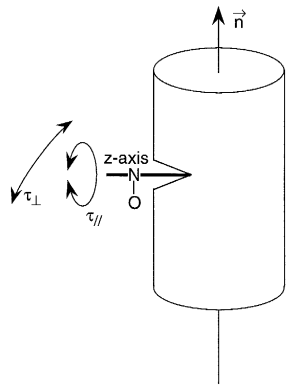

Fig. 5. Schematic model of the motion of the maleimide spin label attached to the cysteine of the M13 coat protein mutant (A25C/A27S) in a lipid bilayer. It is assumed that the local spin-label motion is within a conical cleft at the surface of the coat protein. The local anisotropic spin label motion is described by the motion about the principal *z*-axis ($\tau_{\parallel}$) of the spin label and a wobbling motion of the principal *z*-axis itself ($\tau_{\perp}$). The top angle of the cone is about 23° (not to scale) as calculated from the order parameter ($S = 0.94$) of the spin label. The transmembrane protein part is parallel to the normal **n** to the lipid bilayer. The correlation time $\tau_{\perp}$ for the wobbling motion is affected by the rotational motion of the coat protein about the normal. It should be noted that the maleimide spin label has only a rotational freedom about the S-C and N-C bonds, which gives rise to a strong motional anisotropy.

Thus the basic idea of the motional model in Fig. 5 is that the wobbling motion of the principal *z*-axis with a correlation time $\tau_{\perp}$, mainly arises from the anisotropic motion of the coat protein about the membrane normal. Therefore, based on the results in Fig. 4 we interpret the spectra as a wobbling motion with a correlation time $\tau_{\perp}$ of about 10^{-6} to 10^{-5} s and a relatively fast motion of the spin label about its long molecular axis (principal *z*-axis), with a correlation time $\tau_{\parallel}$ of about 10^{-7} s.

Since the wobbling motion describes the rotational motion of M13 coat protein about the bilayer normal, this allows us to make an estimate of $\tau_{\perp}$. Based on an approximately cylindrical conformation of the transmembrane protein part [16], $\tau_{\perp}$ can be described by

$$\tau_{\perp} = 1/\left(3D_{\mathrm{R}} \sin^2\theta\right), \qquad (1)$$

where θ is the angle between the nitroxide *z*-axis and the protein rotation axis, which is about 90° (see Fig. 5), and D_{R} is the rotational diffusion coefficient of M13 coat protein around its own axis, which is given by [35]

$$D_{\mathrm{R}} = kT/4\pi\eta a^2 h. \qquad (2)$$

The height and radius of the cylinder are $h \approx 3.5$ nm and $a \approx 0.5$ nm, respectively [16], k is Boltzmann's constant, T the absolute temperature. Taking $\eta = 0.37$ Pa · s for the membrane viscosity of 1,2-dimyristoyl-*sn*-glycero-3-phosphocholine (DMPC) just above the gel to liquid crystalline phase transition temperature [35], this gives an estimate for $\tau_{\perp}$ of 3.4×10^{-7} s at 20°C. It may be expected that the membrane viscosity of DOPC (which has a liquid crystalline phase transition temperature of −16°C [36]) at this temperature is lower, so the calculated value of $\tau_{\perp}$ is an upper estimate.

The calculated value of $\tau_{\perp}$ (3.4×10^{-7} s at 20°C), using Eq. (1) and Eq. (2), is a factor of 10 smaller as

compared to the value of 3.5×10^{-6} s obtained from Fig. 4A at L/P 65 and a temperature of 20°C. Also the increase of $\tau_\perp$ with decreasing temperature from 30 to 10°C is not well described by Eq. (1) and Eq. (2). In Fig. 4A it can be seen that at L/P 65 the increase is a factor of 16. The model predicts that $\tau_\perp$ is proportional to η/T (see Eq. (1) and Eq. (2)), and it is unlikely that this factor will account for this effect. This indicates that Eq. (1) and Eq. (2) do not well describe the actual rotational motion of the protein in the bilayer.

One explanation could be that the protein in the bilayer increases the local viscosity η in Eq. (2). An indication for this effect is the continuous increase of $\tau_\perp$ at all temperatures with increasing protein concentrations in the bilayer systems, i.e. by decreasing L/P ratio. At L/P ratios below 15, $\tau_\perp$ strongly increases (see Fig. 4A), and the EPR spectra show a steep increase in line broadening and increase of outer hyperfine splitting $2A_{zz}$ (see Fig. 2). At an L/P ratio of 12, the protein is covered by only one phospholipid layer, and this reduction in protein motion could indicate direct protein-protein interactions. This effect has also been observed with fatty acid spin labels [15]. Another possibility is that the protein is able to aggregate and form reversible protein complexes by hydrophobic interaction. By this effect, the volume factor a^2h in Eq. (2) will increase, giving rise to an increase of $\tau_\perp$.

Alternatively it is conceivable that the N-terminal part does not extend outside the bilayer with an orientation perpendicular to the lipid bilayer surface, but makes an angle with the bilayer normal. It could even be in an orientation parallel to the membrane surface, as has been suggested for fd coat protein [9]. Such an orientation of the N-terminal region would increase the apparent diameter of the membrane-bound coat protein by roughly a factor of 3 and increase $\tau_\perp$ by a factor of about 10. Taking into account a bent protein configuration, it could be possible that the N-terminal part of the M13 coat protein changes from a more extended structure at high temperature to a more tilted structure at lower temperature. This would increase the apparent diameter of the coat protein in Eq. (2), thereby progressively increasing $\tau_\perp$. This could explain the failure of Eq. (1) and Eq. (2) to describe the temperature dependence of $\tau_\perp$.

Apart from this, it should be mentioned that in the analysis of the ST-EPR spectra, a reference set of isotropic rotating spin labels is used for an anisotropic motion. This could give rise to a systematic error in the experimental value of $\tau_\perp$. An indication for such a systematic error is found in the value of $\tau_\perp$ derived from H″/H, which is about 10^{-5} s, which is for most of the cases larger than the value found from the ratio L″/L. Also from the spread of the data points in Fig. 4, it can be seen that there are relatively large errors involved in the experimental determination of $\tau_\perp$.

In Fig. 4B it can be seen that the effect of temperature and L/P ratio on the motion of the spin label about the principal *z*-axis ($\tau_\parallel$) is much smaller as compared to $\tau_\perp$. The indicates that this motion is relatively independent of the local spin label environment, given by the phospholipids and other protein molecules. Thus the lipids and proteins in the bilayer do not restrain this motional freedom of the spin label.

Another possible explanation of the EPR results would be that the spin label *z*-axis is aligned parallel to the membrane normal, with the protein rotating about the normal. We can exclude this possibility for the following reasons.

(1) If the spin label *z*-axis would be oriented along the membrane normal, this would require a very rigid attachment of the spin label via the cysteine side

Fig. 6. Molecular models of maleimide spin-labeled mutant M13 coat protein (A25C/A27S). Side view (top left) and view from bottom (bottom left) of the amino acid region from Ala16 (top) to Gly34 (bottom) in an assumed α-helical conformation. Side view (top right) and view from bottom (bottom right) of the amino acid region from Asn12 (top) to Gly34 (bottom) with a β-turn structure from Gly23 to Glu20; the remaining protein part is in an α-helical conformation. The maleimide spin label is shown in balls and sticks. Plots were made with MOLSCRIPT [42]. The modeling was carried out using the standard parameter set of the computer programme Insight II (Biosym Technologies, San Diego, CA, USA) and standard commands were used. For the extended structure an α-helix was constructed from amino acid 1–50. In the case of the L-shaped structure, an α-helix was constructed from amino acid 1–19 and 24–50, and a 1,4 β-turn structure of type B2 [29] from amino acid 20–23.

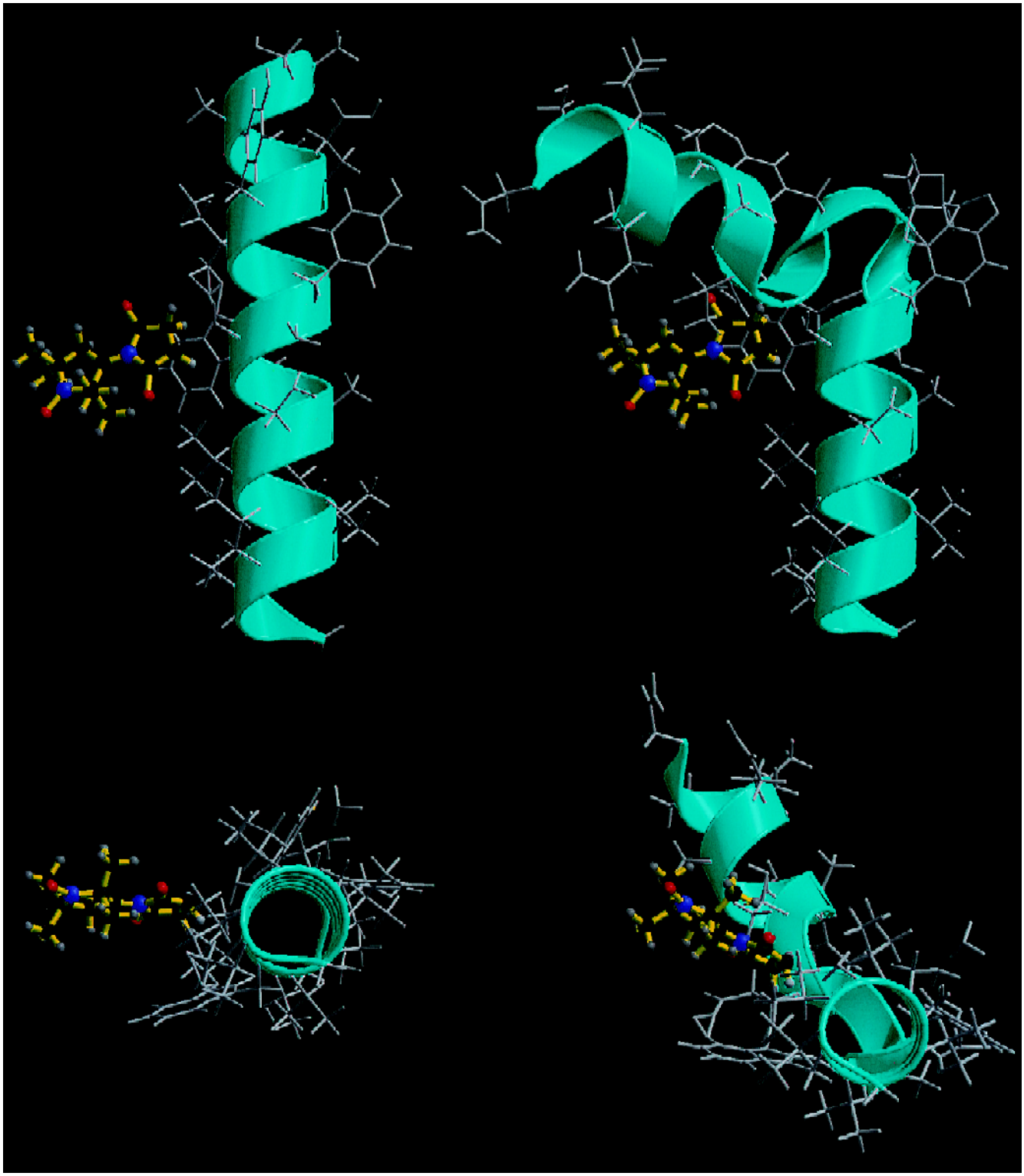

chain to the protein backbone (no local motion). However, for CCMV coat protein it has been found that such an anisotropic motion is possible [32,34], whereas molecular modeling of spin-labeled M13 coat protein shows a relatively high local flexibility (see discussion in relation to Fig. 6). In fact, quite different EPR spectra indicative for much more motion are recorded for other M13 coat protein mutants in phospholipid systems [37].

(2) If the spin label z-axis would be aligned parallel to the membrane normal, all motional effects would come from the anisotropic motion of the coat protein molecule about the protein long axis ($\tau_{\parallel}$), and a protein wobble ($\tau_{\perp}$). From Fig. 4 we then obtain $\tau_{\perp} \approx 10^{-6}$–$10^{-5}$ s and $\tau_{\parallel} \approx 10^{-7}$ s. Now, using Eq. (1), and realizing that to a good approximation $\theta = 23/2 = 11.5°$, and that Eq. (1) now describes the protein long axis motion given by $\tau_{\parallel}$, $\tau_{\parallel}$ turns out to be $3.4 \times 10^{-7}/\sin^2\theta = 8.5 \times 10^{-6}$ s at 20°C. This is about a factor 100 too slow as found experimentally. All the other factors that are discussed in relation to Eq. (1) increase this factor even more. Therefore, this analysis shows that $\tau_{\parallel}$ is too small to describe the overall anisotropic protein motion, and thus must be related to a local spin label motion.

From the estimated order parameter (0.94) it can be calculated that the total cone angle is about 23°. This angle is much smaller than the value found for maleimide spin-labeled coat protein of CCMV ($\approx$ 80°) [32]. This indicates that the spin label experiences a strong squeezing effect by its local environment, that effectively reduces the amplitude of the wobbling motion.

To get an insight in the environment of the spin label attached to mutant M13 coat protein (A25C), we have built a molecular model of maleimide spin-labeled coat protein using the standard parameter set and commands of the computer programme Insight II. One possibility is the assumption of an α-helical protein conformation around amino acid position 25, as found from NMR experiments [9,10]. The aromatic amino acid residues Trp26 and Tyr24 are located in the direct vicinity of the spin label. To see whether the spin label can be stacked between these two aromatic residues, the distances between the spin label and these residues were evaluated. For the protein in an α-helical conformation, it can be observed that the spin label is sticking out of the protein backbone in the hydrophobic lipid region with its long axis oriented almost perpendicular to the protein backbone. This is illustrated in Fig. 6 (left side), showing a side and bottom view of the relevant part of the coat protein. The minimum distance of the maleimide ring of the spin label to Trp26 is around 0.5 nm, but the distance with respect to the nitroxide ring is much larger. The minimum distance of the label with respect to Tyr24 is larger than 0.5 nm. The same is true for all other amino acid residues. Therefore stacking of the spin label by Tyr24, and Trp26 is not likely. The spin label is sticking out quite far from the protein backbone and is expected to have a relatively large amplitude for the wobbling motions. This is not consistent with the high order parameter ($S = 0.94$).

In principle, it should be possible to quantitate the wobbling motion of the spin label from the molecular model in terms of a cone angle, and compare this with the results obtained from the order parameter. However, the model provided by the computer programme Insight II is too limited and does not allow to get such a result. More advanced models, such as molecular dynamics are not yet available for the time scales of motion in our system.

FT-IR spectroscopy on M13 coat protein reconstituted in phospholipid systems suggests a large amount of turn structure (46%). This turn structure is proposed to resemble a discontinuous α-helix, which is located mainly in the C- and N-terminal regions of the coat protein [38]. There is strong evidence that, when going from the inner part of the membrane to the N-terminal part, Tyr24 is the last amino acid residue of the transmembrane α-helix [8–10,39,40]. Taking into account that glycine often acts as an α-helix breaker, a turn structure could start from Gly23. Fig. 6 (right side) show a side view and bottom view of a molecular model of the spin-labeled mutant coat protein containing a 1,4 β-turn structure of type B2 [29] from Gly23 to Glu20, whereas the remaining part of the protein is in an α-helical conformation. The β-turn represents the third most important structural element of peptides and proteins. In this conformation the distance between the C=O group and the N-H group of Glu20 and Gly23 is close enough to form a hydrogen bond. By this effect, the spin label is clearly squeezed by the L-shaped backbone of the protein, giving a reduction

of the motional amplitude for the wobbling motion. For example, the distance of the spin label to the backbone around Glu20 is at some points less than 0.5 nm. Furthermore, it should be noted that the maleimide spin label has only a rotational freedom about the S-C and N-C bonds, giving a relatively small internal flexibility, which gives rise to a strong motional anisotropy.

In discussing the experimental and theoretical values of $\tau_{\perp}$, it was also found that Eq. (1) and Eq. (2) do not well describe the rotational motion of the coat protein mutant in the bilayer, and that this could be due to a tilted orientation of the N-terminal part. This is consistent with the interpretation of the motional amplitude, leading to a turn structure from Gly23 to Glu20. The location of this turn structure is in good agreement with the proposed hinge region around Ile22 [10]. Furthermore, is conceivable that Ile22 is in the central part of a turn, sticking out its bulky side chain. This makes it very unlikely that Ile22 is a starting amino acid residue for a turn in the region from Thr19 to Ile22. In the region from Glu20 to Gly23, also other 1,4 turn structures have been investigated. However, only in the case of a 1,4 hydrogen-bonded turn structure, the distance of the maleimide spin label to the protein backbone is close enough for a squeezing effect.

In conclusion, modeling shows that in an extended protein conformation the spin label has a relatively large amplitude of motion. This is not consistent with the high order parameter ($S = 0.94$). Also it shows that aromatic side chains close to the spin label can not affect the amplitude of motion. The only way to get a reduction of the motional amplitude is by invoking a bent structure with a turn from Glu20 to Gly23. In this case, the spin label at position 25 can be squeezed between the N-terminal and the transmembrane protein parts. For turn structures, infrared frequencies different from those of α-helices are found, depending on the dihedral angles of the turn [41]. It is therefore conceivable that the 1,4 hydrogen-bonded β-turn structure proposed for M13 coat protein is responsible for the specific low-frequency band around 1635 cm^{-1} in the FT-IR spectra of lipid-bound M13 coat protein that has been assigned to hydrogen-bonded turn [38].

Acknowledgements

This research was supported by the Netherlands Foundation of Chemical Research with financial aid of the Netherlands Organization for Scientific Research (NWO) and by the commission of the European Communities, contract nr. ST2J-0088.

References

[1] R.E. Webster, J. Lopez, Structure and Assembly of the Class I Filamentous Bacteriophage, Jones and Bartelett Publishers Inc., Boston, MA, 1985.
[2] I. Rasched, E. Oberer, Microbiol. Rev. 50 (1986) 401–427.
[3] P. Model, M. Russel, In: R. Calendar (Ed.), The Viruses: The Bacteriophages, Vol. 2, Plenum Press, New York, NY, 1988, pp. 375-456.
[4] M. Russel, Mol. Microbiol. 5 (1991) 1607–1613.
[5] M.A. Hemminga, J.C. Sanders, R.B. Spruijt, In: H. Sprecher (Ed.), Progress in Lipid Research, Vol. 31, Pergamon Press, Oxford, 1992, pp. 301-333.
[6] M.A. Hemminga, J.C. Sanders, C.J.A.M. Wolfs, R.B. Spruijt, in: A. Watts (Ed.), Protein-Lipid Interactions, New Comprehensive Biochemistry, Vol. 25, Elsevier, Amsterdam, 1993, pp. 191-212.
[7] R.B. Spruijt, M.A. Hemminga, Biochemistry 30 (1991) 11147–11154.
[8] G.D. Henry, B.D. Sykes, Biochemistry 31 (1992) 5284–5297.
[9] P.A. McDonnell, K. Shon, Y. Kim, S.J. Opella, J. Mol. Biol. 233 (1993) 447–463.
[10] F.J.M. Van de Ven, J.W.M. Van Os, J.M.A. Aelen, S.S. Wymenga, M.L. Remerowski, R.N.H. Konings, C.W. Hilbers, Biochemistry 32 (1993) 8322–8328.
[11] C.H.M. Papavoine, R.N.H. Konings, C.W. Hilbers, F.J.M. Van de Ven, Biochemistry 33 (1994) 12990-12997.
[12] E. Thiaudière, M. Soekarjo, E. Kuchinka, A. Kuhn, H. Vogel, Biochemistry 32 (1993) 12186–12196.
[13] J.C. Sanders, T.W. Poile, R.B. Spruijt, N.A.J. van Nuland, A. Watts, M.A. Hemminga, Biochim. Biophys. Acta 1066 (1991) 102–108.
[14] J.C. Sanders, T.W. Poile, C.J.A.M. Wolfs, M.A. Hemminga, Biochim. Biophys. Acta 1110 (1992) 218–224.
[15] J.C. Sanders, M.F. Ottaviani, A. van Hoek, A.J.W.G. Visser, M.A. Hemminga, Eur. Biophys. J. 20 (1992) 305–311.
[16] H.H.J. De Jongh, M.A. Hemminga, D. Marsh, Biochim. Biophys. Acta 1024 (1990) 82–88.
[17] C. Altenbach, T. Marti, H.G. Khorana, W.L. Hubbell, Science 248 (1990) 1088–1092.
[18] M.S. Weiss, U. Abele, J. Weckesser, W. Welte, E. Schiltz, G.E. Schulz, Science 254 (1991) 1627–1630.

[19] J. Deisenhofer, O. Epp, K. Miki, R. Huber, H. Michel, Nature 318 (1985) 618–624.
[20] R. Henderson, J.M. Baldwin, T.A. Ceska, F. Zemlin, E. Beckmann, K.H. Downing, J. Mol. Biol. 213 (1990) 899–929.
[21] J. Tommassen, In: J.A.F. Op den Kamp (Ed.), NATO Advanced Science Institutes Series, Vol. Series H: Cell Biology, Vol. 16: Membrane Biogenesis, Springer Verlag, Berlin, 1988, pp. 352-373.
[22] J. Sambrook, E.F. Fritsch, T. Maniatis, Molecular Cloning, Cold Spring Harbor Laboratory Press, New York, 1989.
[23] R.B. Spruijt, C.J.A.M. Wolfs, M.A. Hemminga, Biochemistry 28 (1989) 9158–9165.
[24] S. Makino, J.L. Woolford Jr., C. Tanford, R.E. Webster, J. Biol. Chem. 250 (1975) 4327–4332.
[25] D.D. Thomas, L.R. Dalton, J.S. Hyde, J. Chem. Phys. 65 (1976) 3006–3024.
[26] M.A. Hemminga, Chem. Phys. Lipids 32 (1983) 323–383.
[27] M.A. Hemminga, P.A. De Jager, D. Marsh, P. Fajer, J. Magn. Reson. 59 (1984) 160–163.
[28] M.A. Hemminga, J.H. Reinders, P.A. De Jager, J. Magn. Reson. 58 (1984) 428–441.
[29] P.Y. Chou, G.D. Fasman, J. Mol. Biol. 115 (1977) 135–175.
[30] H.O. Griffith, P.C. Jost, In: L.J. Berliner (Ed.), Spin Labeling. Theory and Applications, Academic Press, New York, San Francisco, London, 1976, pp. 453-523.
[31] D. Marsh, Mol. Biol., Biochem. Biophys. 31 (1981) 51–142.
[32] M.A. Hemminga, A.J. Faber, J. Magn. Reson. 66 (1986) 1–8.
[33] A.R. Khan, K.A. Williams, J.M. Boggs, C.M. Deber, Biochemistry 34 (1995) 12388–12397.
[34] G. Vriend, J.G. Schilthuis, B.J.M. Verduin, M.A. Hemminga, J. Magn. Reson. 58 (1984) 421–427.
[35] R.J. Cherry, R.E. Godfrey, Biophys. J. 36 (1981) 257–276.
[36] P.W.M. Van Dijck, B. De Kruijff, L.L.M. Van Deenen, J. De Gier, R.A. Demel, Biochim. Biophys. Acta 455 (1976) 576–587.
[37] D. Stopar, R.B. Spruijt, C.J.A.M. Wolfs, M.A. Hemminga, Biochemistry 35 (1996) 15467–15473.
[38] W.F. Wolkers, P.I. Haris, A.M.A. Pistorius, D. Chapman, M.A. Hemminga, Biochemistry 34 (1995) 7825–7833.
[39] Z.M. Li, C.M. Deber, Biochem. Biophys. Res. Commun. 180 (1991) 687–693.
[40] R.B. Spruijt, C.J.A.M. Wolfs, J.W.G. Verver, M.A. Hemminga, Biochemistry 35 (1996) 10383–10391.
[41] H.H. Mantsch, A. Perczel, M. Hollosi, G.D. Fasman, Biopolymers 33 (1993) 201–207.
[42] P.J. Kraulis, J. Appl. Cryst. 24 (1991) 946–950.